

AD-A070 344

COMPUTERIZED PATTERN RECOGNITION APPLIED TO NI-CD CELL
LIFETIME PREDICTION(U) PURDUE UNIV LAFAYETTE IND DEPT
OF CHEMISTRY W A BYERS ET AL. AUG 78 TR-1

1/1

UNCLASSIFIED

N00014-77-C-0353

F/G 10/3

NL





MICROCOPY RESOLUTION TEST CHART
NATIONAL BUREAU OF STANDARDS-1963-A

AD-A070344

OFFICE OF NAVAL RESEARCH

Contract No. N00014-77-C-0353

Task No. NR 359-650

TECHNICAL REPORT NO. 1

COMPUTERIZED PATTERN RECOGNITION
APPLIED TO Ni - Cd CELL LIFETIME PREDICTION

by

W. Arthur Byers and S. P. Perone*

Purdue University
Department of Chemistry
W. Lafayette, IN 47907

Prepared for publication in

J. Electrochemical Society

August, 1978

Reproduction in whole or in part is permitted for
any purpose of the United States Government

Approved for Public Release; Distribution Unlimited

Unclassified

SECURITY CLASSIFICATION OF THIS PAGE (When Data Entered)

| REPORT DOCUMENTATION PAGE | | READ INSTRUCTIONS BEFORE COMPLETING FORM |
|---|-----------------------|--|
| 1. REPORT NUMBER Technical Report No. 1 | 2. GOVT ACCESSION NO. | 3. RECIPIENT'S CATALOG NUMBER |
| 4. TITLE (and Subtitle) Computerized Pattern Recognition Applied to Ni-Cd Cell Lifetime Prediction | | 5. TYPE OF REPORT & PERIOD COVERED Interim |
| 7. AUTHOR(s) W. Arthur Byers and S. P. Perone | | 6. PERFORMING ORG. REPORT NUMBER |
| 9. PERFORMING ORGANIZATION NAME AND ADDRESS Purdue University Department of Chemistry W. Lafayette, IN 47907 | | 8. CONTRACT OR GRANT NUMBER(s) N00014-77-C-0353 |
| 11. CONTROLLING OFFICE NAME AND ADDRESS Materials Science Division Office of Naval Research Arlington, VA 22217 | | 10. PROGRAM ELEMENT, PROJECT, TASK AREA & WORK UNIT NUMBERS NR 359-650 |
| 14. MONITORING AGENCY NAME & ADDRESS (if different from Controlling Office) | | 12. REPORT DATE August, 1978 |
| | | 13. NUMBER OF PAGES 28 |
| | | 15. SECURITY CLASS. (of this report) Unclassified |
| | | 15a. DECLASSIFICATION/DOWNGRADING SCHEDULE |
| 16. DISTRIBUTION STATEMENT (of this Report) Approved for Public Release; Distribution Unlimited | | |
| 17. DISTRIBUTION STATEMENT (of the abstract entered in Block 20, if different from Report) | | |
| 18. SUPPLEMENTARY NOTES Submitted for publication in <u>J. Electrochemical Society</u> | | |
| 19. KEY WORDS (Continue on reverse side if necessary and identify by block number) Pattern Recognition Battery Testing Battery Lifetime Prediction Cluster Analysis | | |
| 20. ABSTRACT (Continue on reverse side if necessary and identify by block number) Computerized pattern recognition was used to look for characteristics of new nickel-cadmium spacecraft cells which would be predictive of later performance under stressful conditions. It was found that the changes in voltage while a cell was being charged could be used to make a rough estimate of its lifetime. The standard deviation in the predicted lifetime values was somewhat smaller than the standard deviation of the lifetime distribution as a whole, and there are indications that a more extensive data set would yield better results. | | |

DD FORM 1473

1 JAN 73

EDITION OF 1 NOV 68 IS OBSOLETE
S/N 0102-014-6001Unclassified
SECURITY CLASSIFICATION OF THIS PAGE (When Data Entered)

ABSTRACT

Computerized pattern recognition was used to look for characteristics of new nickel-cadmium spacecraft cells which would be predictive of later performance under stressful conditions. It was found that the changes in voltage while a cell was being charged could be used to make a rough estimate of its lifetime. The standard deviation in the predicted lifetime values was somewhat smaller than the standard deviation of the lifetime distribution as a whole, and there are indications that a more extensive data set would yield better results.

When subject to stressful conditions, supposedly identical nickel-cadmium cells will display a wide range of lifetimes. Variations in lifetimes between 50% and 100% are not uncommon for cells which are charged and discharged in an identical manner. The purpose of this work has been to identify characteristics of a cell just off the production line which will be useful in predicting extended performance and time of failure.

Since prediction of battery lifetime is particularly important for spacecraft applications, an extensive testing program for sealed nickel-cadmium cells used in satellites was implemented by NASA at Crane Naval Weapons Support Center in 1974 (1). Cells were subjected to harsh operating conditions to cause accelerated aging and early failure. It was hoped that accelerated testing would be faster and cheaper than the previous practice of testing the cells under conditions identical to what they would encounter on the mission, while producing results which were just as relevant.

Before the cells were cycled to failure at Crane, a series of pre-tests were carried out on them by the manufacturer, General Electric. In these tests, the internal pressures and voltages were recorded at different intervals as the cells were charged and discharged. The length of time it took each cell to discharge to 1.0 volts was also monitored.

We have used several different pattern recognition (2 - 5) techniques to look for relationships between the performance of cells in these pre-tests and their lifetimes. See Table I for a list of features extracted from these tests for use in pattern recognition.

Correlations between the pre-tests done by the manufacturer and the accelerated lifetimes were complicated by the fact that the test program at Crane was factorially designed (6). Eight different test design parameters (factors) were varied over five different levels to show the effect of changes

in cell construction and also to allow extrapolation from the severe testing conditions to normal conditions.

To get information on the effect of design and component changes, 3 of the cell's construction parameters were varied. These were the concentration of the electrolyte, the volume of the electrolyte, and the negative precharge. The possible values for each of these design parameters are given in Table II. There were 14 different combinations of these parameters among the cells that were examined.

To allow for extrapolation of the accelerated results to normal operation the cells were grouped into packs of 5 or 8, and each pack was cycled under conditions different from other packs. Different permutations of the cycling conditions in Table III were used.

The wide range of testing conditions made the comparison of lifetimes between packs difficult. Cells in one pack lasted an average of 18 cycles, while cells in another pack lasted for more than 10,000 cycles. To remove the effect of unwanted variables from the data, the quality of each cell was measured relative only to other cells which had been cycled under identical conditions. Each was assigned a relative lifetime number (RLN) which is defined below:

$$RLN = N/A$$

where, N = # cycles until cell failure

A = average # cycles for all failed cells in the pack.

A cell was considered to have failed if it developed a dangerously high pressure (> 250 psi), was shorted, or would not charge to minimum voltage. Only cells that had failed by June of 1977, and which belonged to packs in which at least two other cells had failed, were included in the analysis. There were 220 such cells.

Two different approaches were taken in a search for tests with predictive information. The first was to use a two-class training set created from the relative lifetime distribution to predict whether a cell would be "good" or "bad", without saying anything about how good or bad it was. The second approach was to use different combinations of tests to make predictions of relative lifetime. The variance of the predicted values from the true values was taken as a measure of the usefulness of the tests used in prediction. Both methods will be described in more detail.

Analysis Using a Two-Class Training Set

Since the results of a predictive test will eventually be used to decide whether or not a cell is adequate for a given application, it seemed reasonable to divide the cells into two classes. A boundary was drawn in a low density region of the relative lifetime distribution, and all cells with lifetimes below the boundary were considered to be "bad". Several different boundaries were tried.

Histograms were then used to look for features in the manufacturer's test which would show a difference in the behavior for good and bad cells. A predictive feature would be indicated if good cells fell in one region of the histogram, and bad cells in another. Such a feature is shown in Figure 1.

No features were found where there was a sharp difference between the good and bad cells. However, it was noticed that there was a high degree of clustering with respect to cell type (the 14 different combinations of design parameters). In an effort to remove this major variation in the data to look at underlying clustering by cell quality, the manufacturer's tests were "type-autoscaled". This means that for each test all the feature values for cells of the same type were pulled out of the distribution,

autoscaled separately, and then returned to the distribution. This procedure eliminated any differences in the magnitude or the standard deviation of the data that were caused by variation in the composition of the cell. This procedure is illustrated for an ideal distribution in Figure 2. (Autoscaling replaces each data point in a distribution with its distance from the mean. The distance is expressed in units of standard deviations. All autoscaled distributions have a mean of 0 and a standard deviation of 1.)

Clustering was also found with respect to the date on which the data were taken. Therefore, the tests were also "date-autoscaled" in a similar manner.

A one-dimensional K-nearest-neighbor analysis was conducted on both the scaled and unscaled data. The features which showed the best classification accuracy were then combined to form a 26-dimensional space. Iterative feature selection (7) was used to improve the K-nearest-neighbor classification accuracy in this space by reduction of dimensionality.

Cluster Analysis

The main problem in the use of two-class pattern recognition for the prediction of cell lifetime is that the results are highly dependent on the initial class definitions, and these definitions were made rather arbitrarily. If the performance of cells falls naturally into three or four classes instead of two, then one may be ignoring a good deal of predictive information by separating the cells into only two classes. To avoid this biasing of the results, a non-parametric hierarchical clustering algorithm was used to examine the natural clustering of the data for certain types of features.

The particular algorithm which was developed seeks out "valleys" in a distribution using the fixed neighborhood classification rule described in Reference 8.

The fixed neighborhood classification rule involves the four following steps:

- 1) Make some initial rough assignment of the clusters.
- 2) For each data point, find all other points within a given fixed radius (r), and determine which clusters those points belong to.
- 3) Assign the point in question to the cluster which has the most members within that radius.
- 4) Continue steps 2 and 3 until no more changes are made in cluster membership.

Several passes through all the data points are usually required before the cluster boundaries settle in low density regions.

Part of the versatility of the algorithm is due to the fact that the choice of r affects the size of the clusters which are formed. A variation of r from small to large values will cause merger of clusters at different levels. This can be used to produce a hierarchical map which shows similarity between clusters.

The initial assignment of clusters is important in that a good first choice can greatly reduce the amount of time required by the algorithm to adjust the cluster boundaries to regions of low density. We have found that most of the common procedures for initial cluster generation are inadequate because they often draw the cluster boundaries in regions of high density, far from the valleys where they eventually end up.

To remedy this problem, a new cluster generation scheme has been implemented which involves the following two steps:

- 1) Each point is assigned to be a cluster generating nucleus.
- 2) The nuclei are sequentially expanded to include their two nearest neighbors, provided that the neighbors are within r .

Using this procedure, initial clusters are always generated in high density regions and execution time for the rest of the program is usually greatly reduced. When compared to a method in which the space was divided into cubes which defined the initial cluster boundaries, the number of passes through the data was reduced by a factor of five.

The algorithm just described was used not only as a tool to examine the characteristics of a space drawn up from a specified set of test features, but also to choose sets of features which optimized the clustering of cells of similar relative lifetimes. It searched for a combination of features which would maximize J , where J is defined in Equation 1. A J value of 100 indicates a perfect predictive feature.

$$J = \frac{\sum_{i=1}^n [1 - (\frac{wcv_i}{BCV})] (100)(n_{c_i})}{n} \quad (1)$$

where, n = # cells

n_{c_i} = # cells in the cluster

wcv_i = variance in relative lifetimes for the cluster

BCV = between cluster variance in relative lifetime.

RESULTS

The k-nearest-neighbor analysis using a two-class training set was not able to find any features in the manufacturer's test data that would give an overall classification accuracy of over 75% for all 220 cells considered together. However, when the cells of each type were separately analyzed, much better results were obtained. For example, when cells designated by Crane as group 4E[†] were looked at alone, it was found that the slope of the voltage vs. time curve (type-and data-autoscaled) as the voltage reached 95% of its maximum value was a good feature for distinguishing between "good" and "bad" cells. Using only feature #16 (ΔV at 8-4 hours) a k-nearest-neighbor analysis correctly classified 90.7% of the cells. This was done with the boundary drawn in the relative lifetime distribution such that 70% of the cells were considered good. Looking at the results in more detail, 93.3% of the good cells were correctly identified, while 84.6% of the bad cells were correctly identified (Table IV). Bad cells were clustered into two groups, one at 0.38 standard deviations from the mean, and the other at -1.33 standard deviations. The K used was 1. See Figure I.

During other cycles of the manufacturer's tests, the cells from group 4E behaved in a similar manner. Feature #23 from the fourth cycle (ΔV at 24-16 hours) again showed a cluster of bad cells at .38 standard deviations.

Results for other cell types are also summarized in Table IV.

[†] Group 4E consisted of cells which had a KOH concentration of 30%, a KOH volume of 19.5 ml. and a precharge of 2.8 amp hours.

The successful classification results obtained when the cell types were looked at individually (Table IV) indicated that the analysis of the entire distribution (after type-autoscaling) gave poor results (75% classification) for reasons other than a lack of lifetime information in the data. Apparently the differences between cell types either caused more than a simple change in the magnitudes of the measurements made by the manufacturer, or else caused some new mode of degradation and failure during the accelerated cycling. In either case, the relationships between the initial tests and the relative lifetime distribution were changed sufficiently for cells of different composition that different features in the manufacturers' tests were useful in prediction of lifetime. It was for this reason that the valley seeking clustering algorithm was used to find cell types which were similar enough in their behavior to be grouped together for the creation of a larger prediction set.

In Figure 3 a hierarcial map produced from the cluster analysis shows which cell types are most similar in a space created from the unscaled cell parameters (precharge, etc.). Each cluster at the base of the map represents a unique type of cell. The cell types have been labeled by the numbers which were assigned to them at Crane (group #).

Another map (Figure 4) was constructed from an 8-dimensional space which was formed from non-autoscaled pressures from the middle of 4 different charging cycles. Note how similar the clustering is to that in cell parameter space. The same smaller clusters, which are composed mostly of cells of identical composition, merge to form 3 major clusters. These larger clusters represent three different manufacturing lots; platelots 1, 2 and 4. This does not necessarily mean that there was a change in the plate/composition between runs, because the clustering in cell parameter space, which only

considered the concentration of electrolyte, the volume of electrolyte and the precharge, also showed 3 major clusters.

Clustering in a 2-D feature space created from features #6 and #12 (the discharge time to 1.0 V) showed clustering by lot number. There were two major clusters, one corresponding to lot 1, and the other to lots 2 and 4 (see Figure 5).

Voltage features were less sensitive to variations caused by cell type. The cells in small clusters were fairly homogeneous in composition, but the marked separation into 3 major cell types at high levels was not as evident. It is perhaps for this reason that voltage features were more useful in prediction than pressure features.

For the clustering at large r , it was postulated that all cells in one lot may behave enough alike to form a common prediction set. To test this hypothesis, cells from lots 1, 2 and 4 were examined separately for clustering by relative lifetime. In large clusters, only clustering by cell type was found, but in the tiny clusters of two or three cells, a fair degree of separation by lifetime was found.

This low level separation into clusters of cells having similar lifetimes is shown in Figure 6. This hierarchical map was produced from a 3-D space constructed from the best features for lot 1. The J value for the smallest clusters was 66.2, so the average within cluster variance in lifetime was only about $1/3$ that for the entire distribution.

Figure 7 shows the low level clustering in the best feature space for lot 4. Here J was 72.8. The features which produced these maps, along with the best features for lot 2 are listed in Table V.

Although clustering by lifetime has been shown, the valley seeking technique used to find the clusters can not be used directly in predicting the lifetime of a new cell. A k-nearest neighbor algorithm in which the lifetimes of a cell's k-nearest neighbors are averaged to predict its lifetime would be better suited. The results of such an analysis using features from Table V are given in Table VI. The restriction that a cell's neighbors must be within a fixed minimum distance was imposed so predictions were not made for all cells.

The k-nearest neighbor results were not as good as might have been expected from the cluster analysis. This was due in part to the crossing of cluster boundaries when large k's were used. Better results were obtained when the lifetime of a cell was predicted to be the mean lifetime of the nearest cluster. It must be remembered, however, that in this case there was some biasing of the results because the cell's lifetime that was being predicted went into making up the mean of the nearest cluster.

Better results were obtained in all cases when the maximum nearest neighbor distance allowed for a prediction was reduced. This is yet another indication that cell quality causes only minor (but significant) variation in the initial performance of a cell, and looking at larger variations will not be helpful.

In Figure 8 the performance of the KNN algorithm for all 220 cells as a function of the maximum neighbor distance has been displayed. The feature space was created from all 8 features listed in Table V. The circles contain the number of cells for which predictions were made. It is easy to see that the deviations of the predictions from the actual relative lifetimes were very small when only cells in high density regions (low maximum NN distances) were considered. Unfortunately there were few cells in these tightly clustered regions.

CONCLUSIONS

Voltage features have been found to be more predictive than pressure features. When all features in which J was greater than 65 and the percentage of cells clustered was greater than 45% were examined, voltage features appeared 36 times compared to 13 times for pressure features. Time required for discharge to 1.0 V was as predictive as the voltages during a charge.

Clustering by cell quality (relative lifetime) is much less pronounced than clustering by other variables such as cell type for the features examined thus far. More precise prediction of cell lifetime will probably require inclusion of detailed knowledge of cell construction and how lifetime is affected by construction variables. It is hoped, however, that the analysis of the shape of better defined charging and discharging curves will yield features which are less dependent on cell type. McDermott and Sommerfeldt have begun such an analysis on curves recorded during the accelerated cycling at Crane, using exponential fit parameters as features (9). No conclusive results are yet available.

When using the best features that have been found so far to test a given type of cell, a good prediction set would require more cells than were used in this analysis. Some cells would fall into empty regions of space so prediction on the basis of their nearest neighbors would be inaccurate.

Few of the features extracted from the data taken toward the end of a charging period were found to be useful. Changes in a cell's voltage and pressure while it is still accepting a charge are much more important than any overcharge phenomenon. Thus, simply recording the final state of a cell after a charge will probably not provide any useful information.

CREDIT

The authors wish to express their gratitude for the financial support of the Office of Naval Research.

ACKNOWLEDGEMENT

The authors would like to thank Don Mains and Louis Goodman for providing the battery test data and Gene Wells, J. R. Birk and William Spindler for their valuable discussions.

REFERENCES

1. NASA/GSFC Document X-761-73-183, Accelerated Test Plan for Nickel-Cadmium Spacecraft Batteries of October, 1973.
2. B. R. Kowalski and C. F. Bender, J. Amer. Chem. Soc., 94, 5632 (1972).
3. T. M. Cover and P. E. Hart, IEEE Transactions on Information Theory, IT-13, 21 (1967).
4. L. Kanal, IEEE Transactions on Information Theory, IT-20, 697 (1974).
5. J. A. Hartigan, "Clustering Algorithms", Wiley, New York (1975).
6. J. P. Elder and E. M. Jost, J. Electrochem. Soc., 116, 687 (1969).
7. M. A. Pichler and S. P. Perone, Anal. Chem., 46, 1790 (1974).
8. K. Fukunaga, "Introduction to Stastical Pattern Recognition", Academic Press, New York, p. 341 (1972).
9. E. E. Sommerfeldt and P. P. McDermott, GSFC Document X-711-77-193, Analysis of Data from the Accelerated Test Program on Aerospace Nickel-Cadmium Cells of July, 1977.

TABLE I.

FEATURES EXTRACTED FROM MANUFACTURER'S PRETEST DATA

| <u>CYCLE</u> | <u>TEST</u> | <u>FEATURES</u> |
|--------------|-----------------------------------|--|
| I | 3.1 Charging at 3.0A | (1) Pressure (t) (2) Δ Pressure (t) (3) Voltage (t) (4) Δ Voltage (t) t = 0, 30, 60, 90, 120, 150 minutes |
| | 3.2 Discharging at 3.0A | (5) Voltage (t) (6) Time to reach 1.0V |
| II | 3.3, 3.4 Identical to 3.1, 3.2 | (7 - 12) Same as 1 - 6 |
| III | 3.5 Charging at 0.75 amps | (13) Pressure (t) (14) Δ Pressure (t) (15) Voltage (t) (16) Δ Voltage (t) t = 4, 8, 12 hours |
| | 3.6 Discharging at 3.0A | (17) Voltage (t) (18) Δ Voltage (t) (19) Time to reach 1.0 Volt t = 60, 120 minutes |
| IV | 4.1 Charging at 0.6A | (20) Pressure (t) (21) Δ Pressure (t) (22) Voltage (t) (23) Δ Voltage (t) t = 0, 8, 16, 24, 32, 40, 48 hours |
| | 4.4 Discharging at 3.0A | (24) Time to Reach 1.0 Volt |

TABLE II

CELL DESIGN PARAMETERS

| | | | | | |
|--------------------------------|------|------|------|------|------|
| Concentration of KOH (%) | 22 | 26 | 30 | 34 | 38 |
| Volume of KOH (ml) | 17.5 | 18.5 | 19.5 | 20.5 | 21.5 |
| Negative Precharge (amp-hours) | 2.20 | 2.50 | 2.80 | 3.00 | 3.30 |

TABLE III

ACCELERATED CYCLING CONDITIONS

| | | | | | |
|------------------------------------|-----|-----|----|----|-----|
| Temperature ($^{\circ}\text{C}$) | 20 | 30 | 40 | 50 | 60 |
| Depth of Discharge (%) | 20 | 40 | 60 | 80 | 100 |
| Charge Rate* | C/4 | C/2 | C | 2C | 4C |
| Discharge Rate* | C/2 | C | 2C | 4C | 8C |

* C = 6 amps

TABLE IV
ANALYSIS OF INDIVIDUAL CELL TYPES

| CELL TYPE (GROUP #) | % GOOD CELLS | # CELLS | BEST FEATURES (ALL DATE AND TYPE AUTOSCALED) SEE TABLE I | TOTAL % CORRECT | % GOOD CORRECT | % BAD CORRECT |
|---------------------------|--------------------|------------|--|-----------------------|----------------------|---------------------|
| 4E | 70 | 40 | #16, ΔV , t = 8 - 4 hours | 90.7 | 93.3 | 84.6 |
| 9 | 68 | 19 | #3, ΔV , t = 30 - 0 min. | 89.5 | 92.3 | 83.3 |
| 10 | 73 | 13 | #22, V, t = 0 hours | 92.3 | 87.5 | 100 |
| 11 | 76 | 17 | BEST SINGLE FEATURE | 88.2 | 83.3 | 100 |
| | | | #13, P, t = 8 hours | | | |
| | | | BEST COMBINATION | 94.1 | 100 | 80 |
| | | | # 7, P, t = 0 minutes | | | |
| | | | #9, V, t = 90 minutes | | | |
| | | | #13, P, t = 8 hours | | | |
| | | | #15, V, t = 4 hours | | | |
| 13 | 77 | 27 | #4, ΔV , t = 30 - 0 minutes | 92.6 | 95.2 | 83.3 |
| | | | #4, ΔV , t = 90 - 60 minutes | " | " | " |
| | | | #8, P, t = 30 minutes | " | " | " |
| 14 | 77 | 13 | #14, ΔP , t = 8 - 4 hours | 100 | 100 | 100 |
| 15 | 65 | 23 | #16, ΔV , t = 8 - 4 hours | 100 | 100 | 100 |
| 16 | 67 | 18 | #12, time discharge to 1.0V | 88.9 | 91.7 | 83.3 |

TABLE V

CLUSTERING RESULTS

Best Predictive Features For Lots 1, 2 and 4

| LOT | AUTOSCALED FEATURE COMBINATIONS | r | % CLUSTERED | J |
|-----|------------------------------------|-----|-------------|------|
| 1 | #23, ΔV at 24 - 16 hrs. | .35 | 81% | 66.2 |
| | #22, V at 32 hrs. | | | |
| | #9, V at 0 hrs. | | | |
| 2 | #9, V at 0 hrs. | .05 | 49% | 68.0 |
| | #12, Time to 1.0V | | | |
| 4 | #9, V at 30 min. | .24 | 68% | 72.8 |
| | #14, ΔP at 8 - 4 hrs. | | | |
| | #10, ΔV at 90 - 60 min. | | | |

TABLE VI

KNN LIFETIME PREDICTION RESULTS

| LOT | K | PREDICTIONS MADE (%) | RLN STANDARD DEVIATION IN LOT | STANDARD DEVIATION IN PREDICTED VALUE |
|-----|---|-------------------------|----------------------------------|--|
| 1 | 7 | 71 | 0.311 | .245 |
| 2 | 5 | 70% | 0.221 | .192 |
| 4 | 7 | 59% | 0.157 | .111 |

LIST OF FIGURES

- Figure 1. This histogram shows the best two-class separation for group 4-E cells. A kNN analysis of this distribution resulted in only 3 misclassifications.
- Figure 2. Type-autoscaling. The procedure has been exemplified for a distribution of only two types of cells. In this study it was used to normalize data from fourteen different cell types.
- Figure 3. Clustering in cell parameter space showing the number of cell types and their similarity. Each line on the figure represents an individual cell.
- Figure 4. Clustering of cells in mid-cycle pressure space. Division of cells into three major clusters similar to the clusters of Figure 3. indicates that the pressure behavior is mainly dependent on variations in the cell construction parameters in Table II.
- Figure 5. Clustering in discharge time space. Note the sharp difference in the behavior of plate lot 1.
- Figure 6. Lifetime clustering in lot 1. See Table V for features.
- Figure 7. Lifetime clustering in lot 4. See Table V for features.
- Figure 8. Change in the standard deviation of predicted lifetime values with maximum nearest neighbor distance allow. At low maximum neighbor distances only tight clusters are considered for lifetime prediction and predictions are more accurate.

FIGURE I

BEST CLASS SEPARATION FOR GROUP 4E

▲ = good cell

● = bad cell



FEATURE 16 ΔV AT T = 8-4 HRS.

(DATE AND TYPE AUTOSCALED)

FIGURE II — TYPE AUTOSCALING

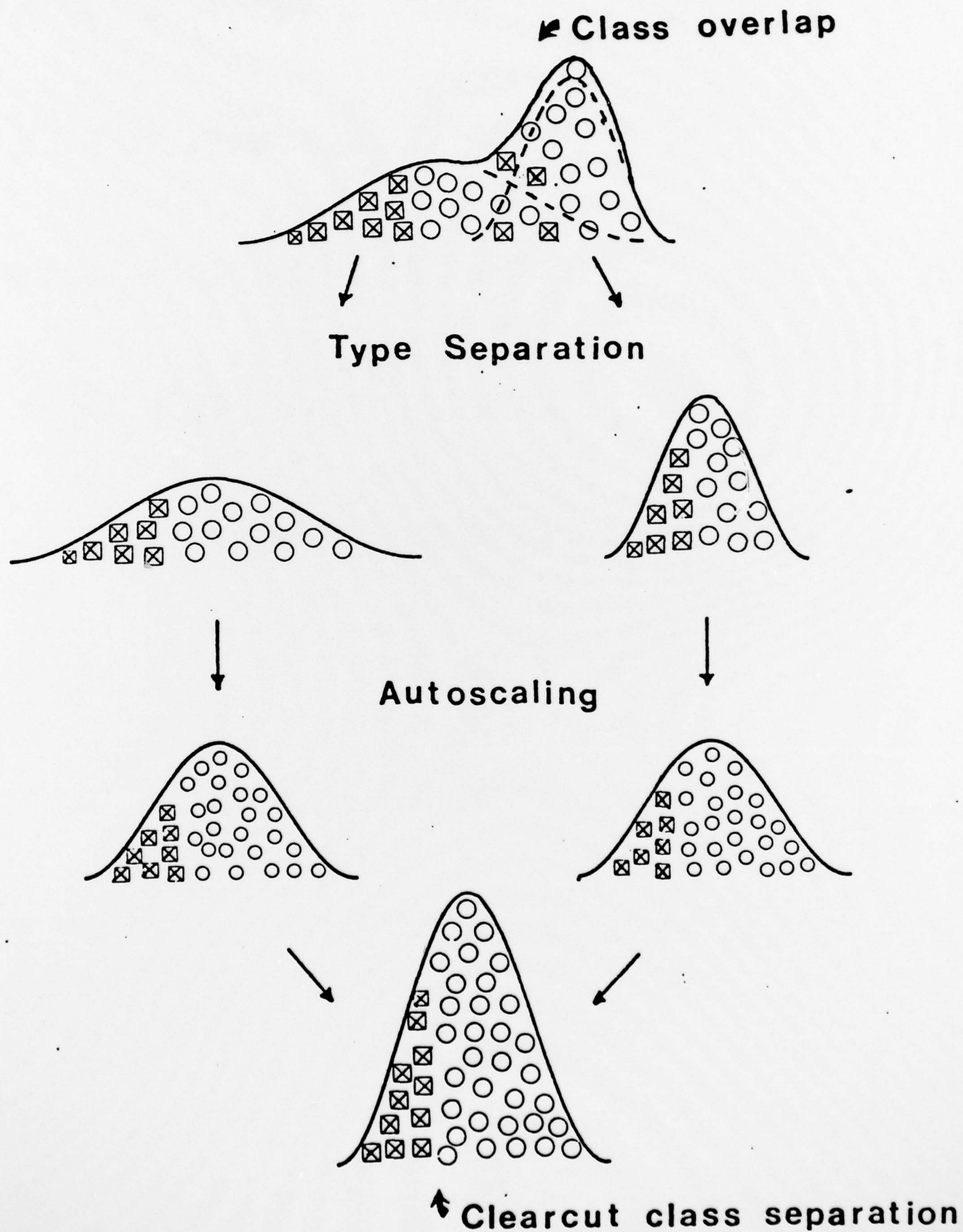


FIGURE III

CLUSTERING IN CELL PARAMETER SPACE

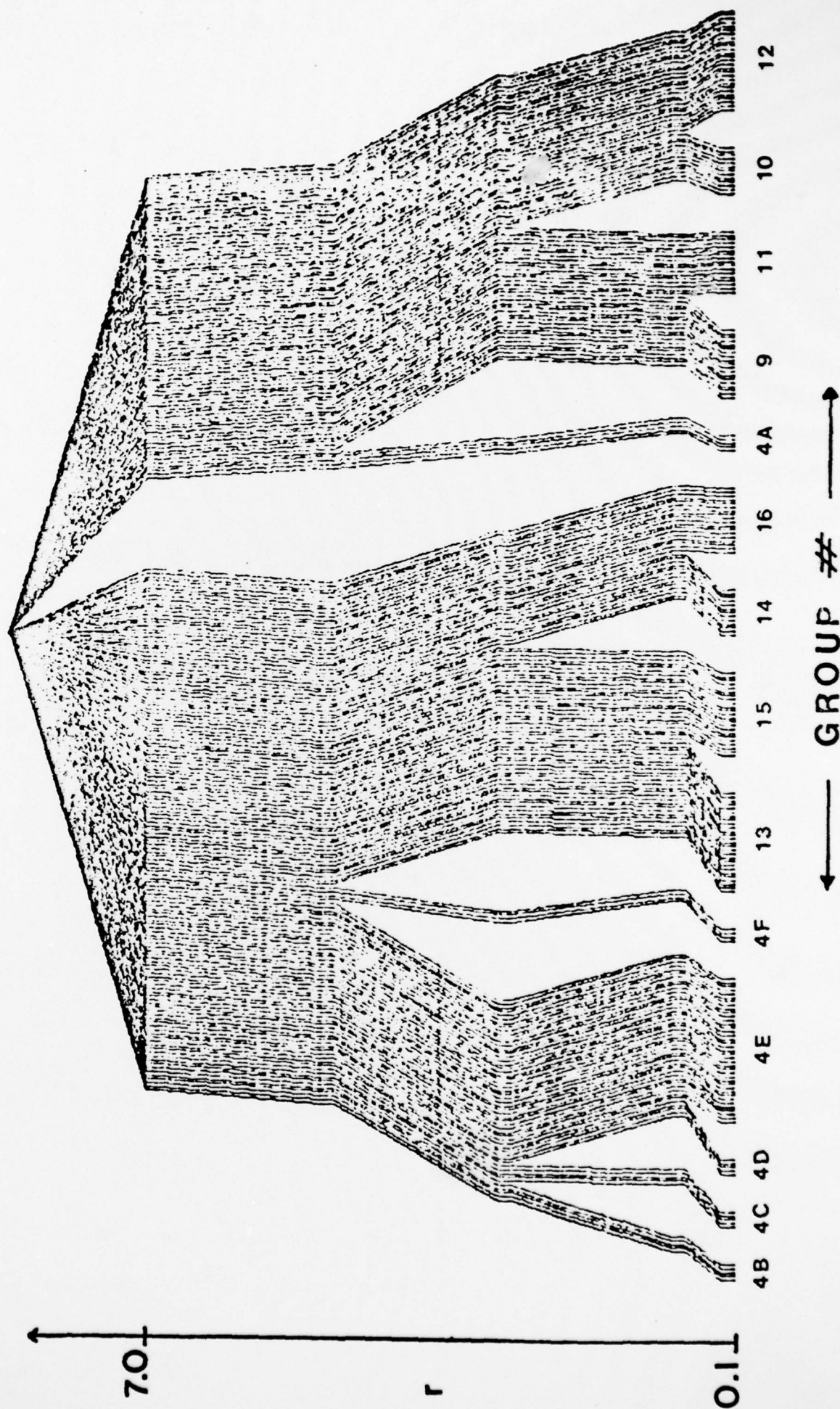


FIGURE IV

CLUSTERING OF CELLS IN MID-CYCLE PRESSURE SPACE

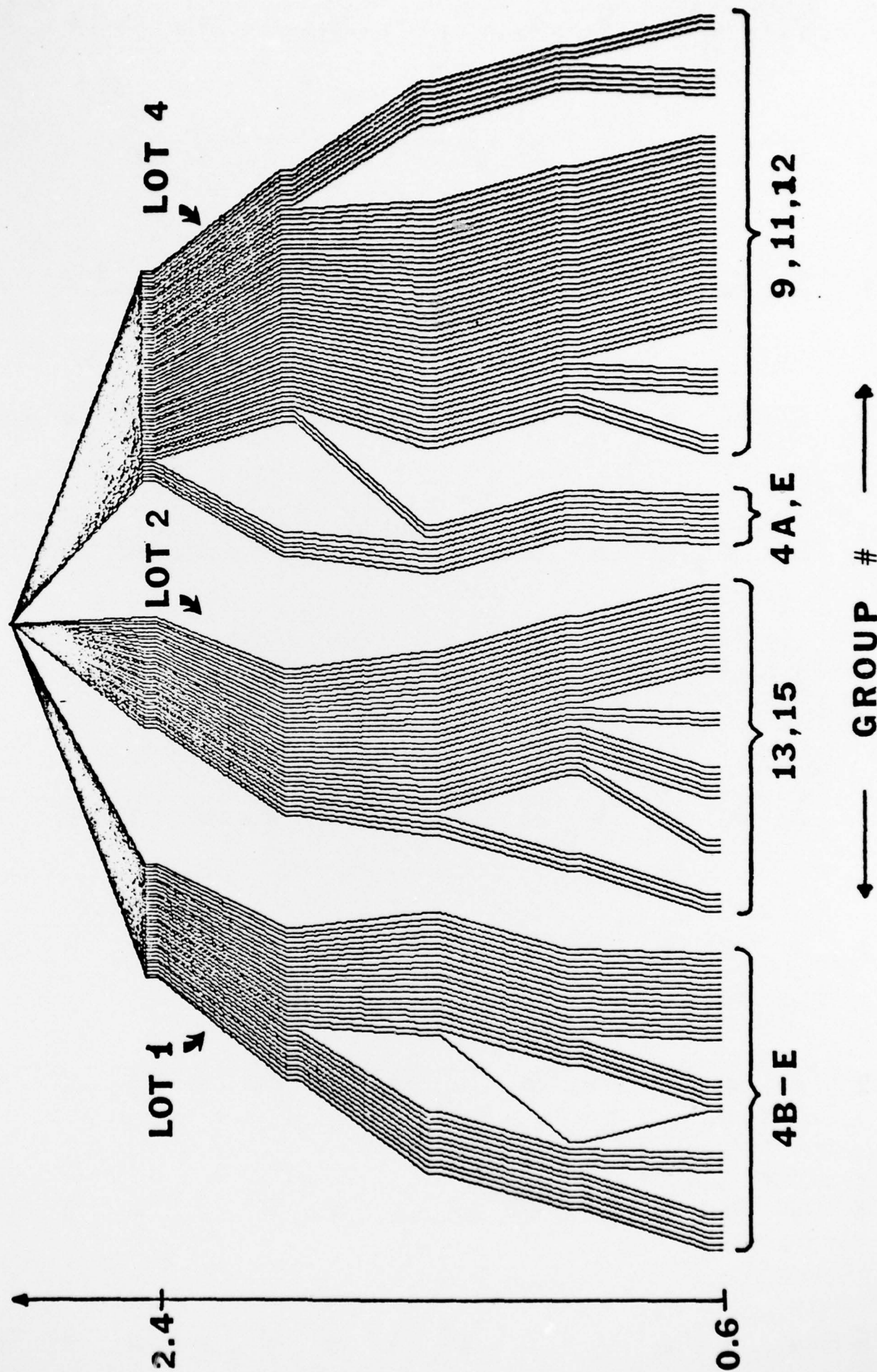


FIGURE V

CLUSTERING IN DISCHARGE TIME SPACE

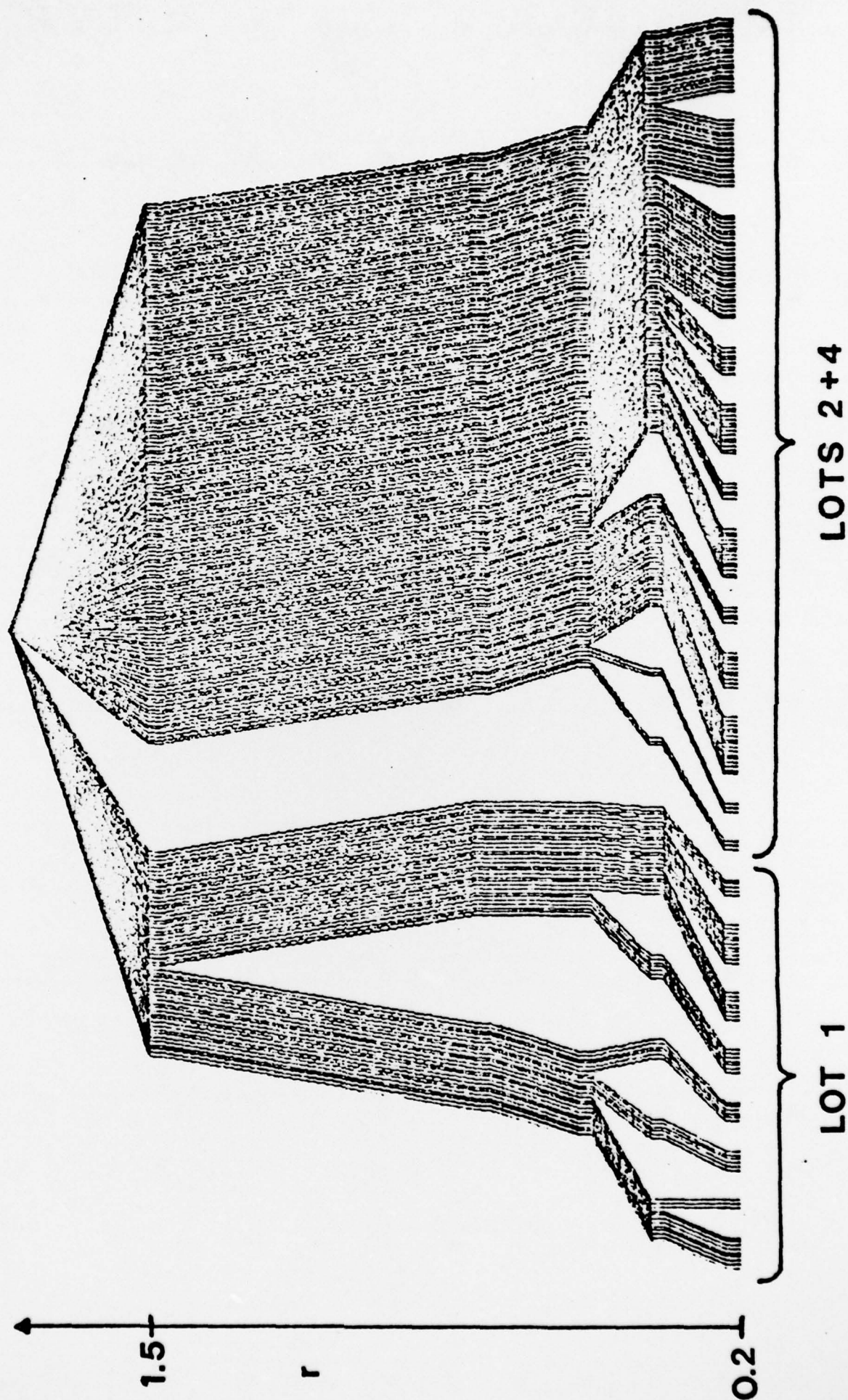


FIGURE VI
BEST FEATURES FOR LOT 1

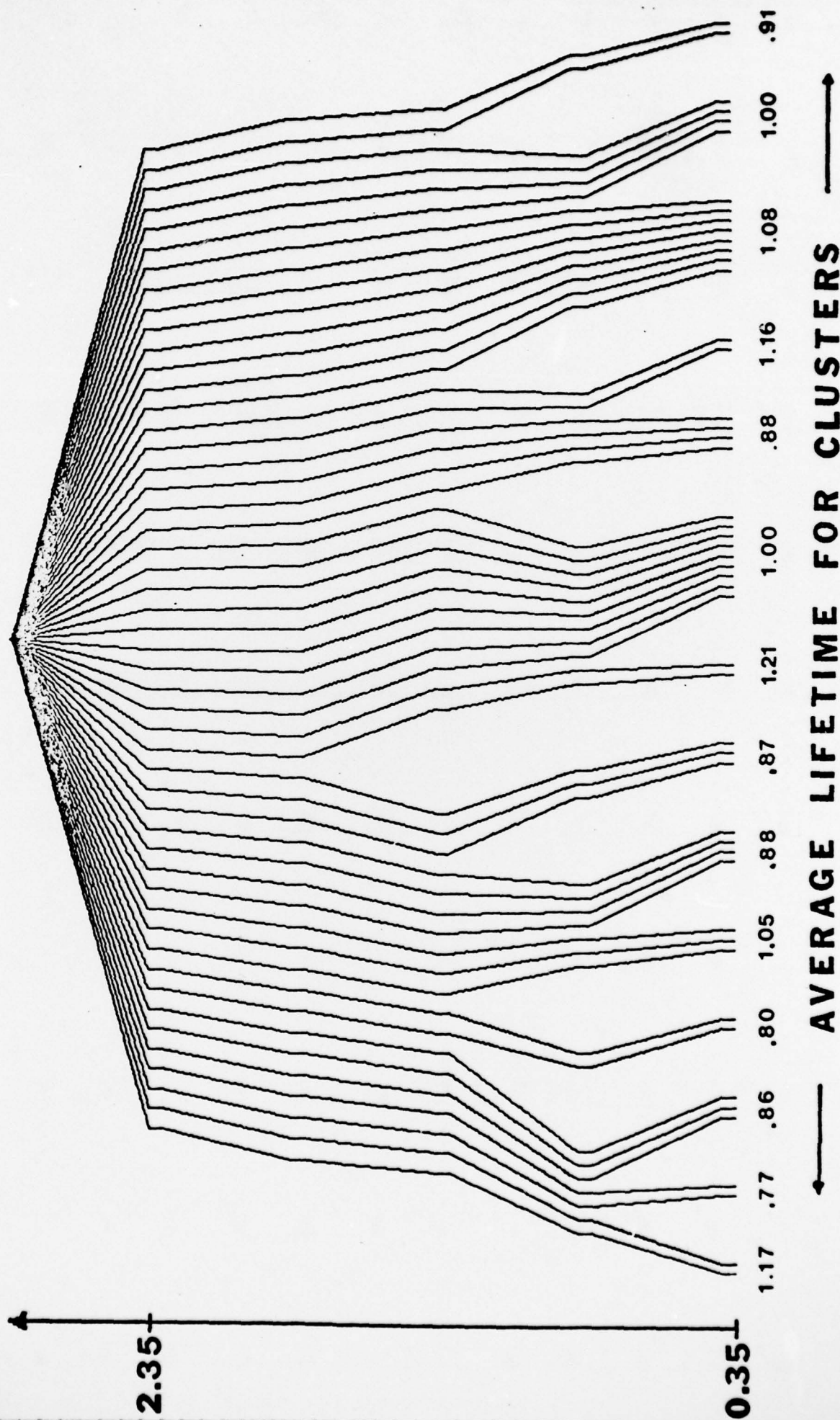


FIGURE VII
BEST FEATURES FOR LOT 4

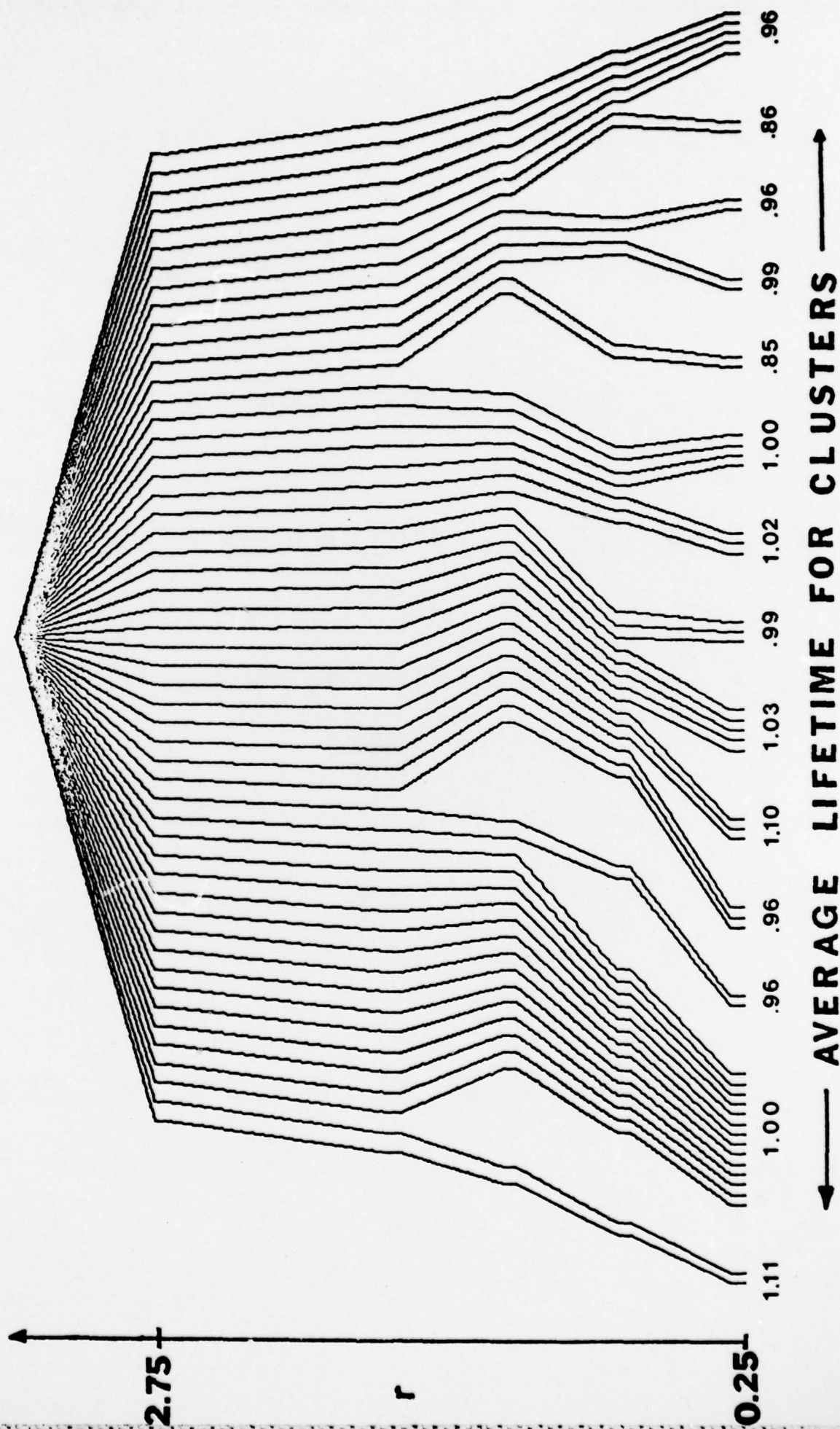
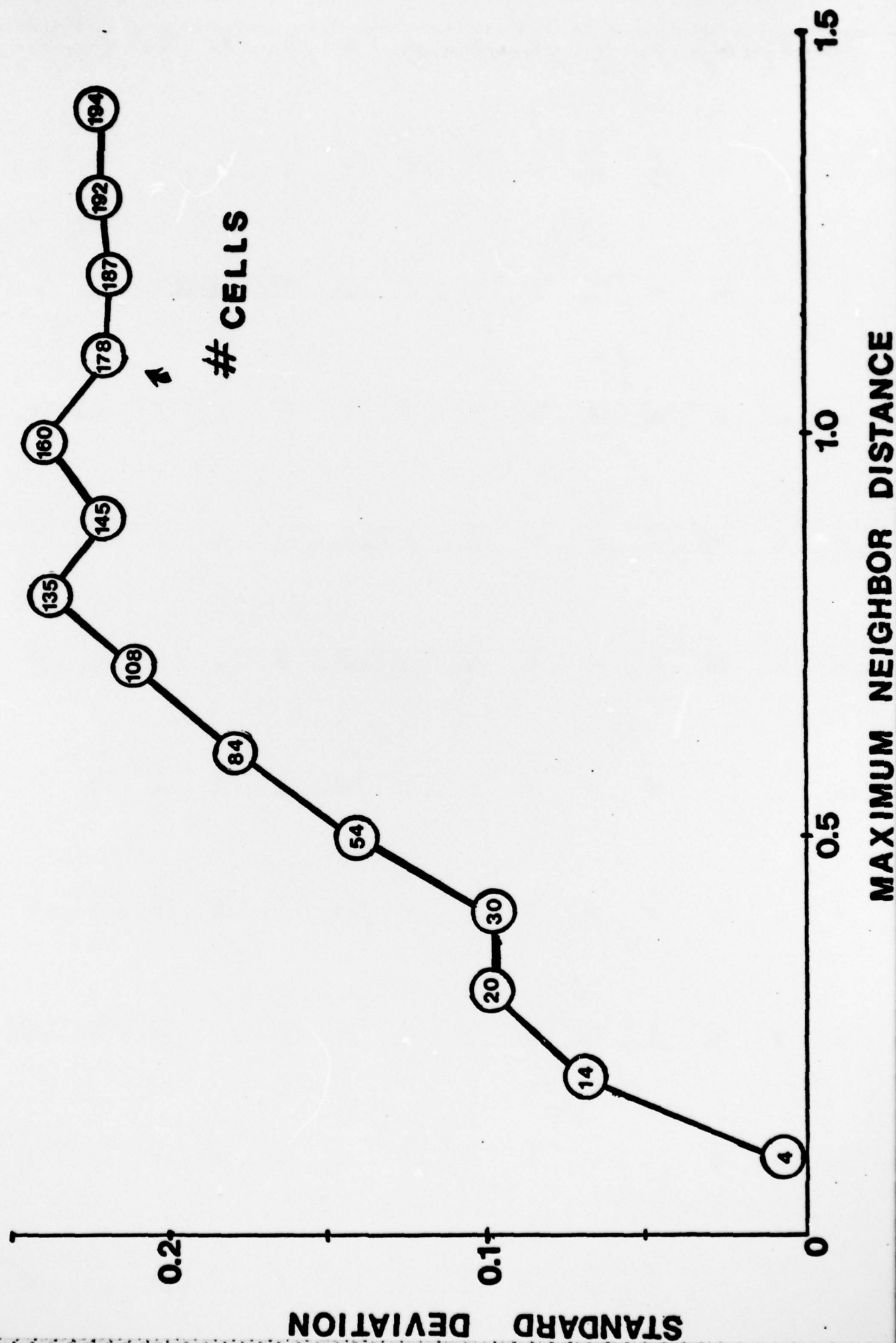


FIGURE VIII

KNN PERFORMANCE FOR ALL CELL TYPES



(Nov, 1971)

Only Batt Testing

NR 259-650

TECHNICAL REPORT DISTRIBUTION LIST

No. Copies

No. Copies

Office of Naval Research
Arlington, Virginia 22217
Attn: Code 472

2

Office of Naval Research
Arlington, Virginia 22217
Attn: Code 102IP 1

6

ONR Branch Office
536 S. Clark Street
Chicago, Illinois 60605
Attn: Dr. Jerry Smith

1

ONR Branch Office
715 Broadway
New York, New York 10003
Attn: Scientific Dept.

1

ONR Branch Office
1030 East Green Street
Pasadena, California 91106
Attn: Dr. R. J. Marcus

1

ONR Branch Office
760 Market Street, Rm. 447
San Francisco, California 94102
Attn: Dr. P. A. Miller

1

ONR Branch Office
495 Summer Street
Boston, Massachusetts 02210
Attn: Dr. L. H. Peebles

1

Director, Naval Research Laboratory
Washington, D.C. 20390
Attn: Code 6100

1

The Asst. Secretary of the Navy (R&D)
Department of the Navy
Room 4E736, Pentagon
Washington, D.C. 20350

1

Commander, Naval Air Systems Command
Department of the Navy
Washington, D.C. 20360
Attn: Code 310C (H. Rosenwasser)

1

Defense Documentation Center
Building 5, Cameron Station
Alexandria, Virginia 22314

12

U.S. Army Research Office
P.O. Box 12211
Research Triangle Park, N.C. 27709
Attn: CRD-AA-IP

1

Naval Ocean Systems Center
San Diego, California 92152
Attn: Mr. Joe McCartney

1

Naval Weapons Center
China Lake, California 93555
Attn: Head, Chemistry Division

1

Naval Civil Engineering Laboratory
Port Hueneme, California 93041
Attn: Mr. W. S. Haynes

1

Professor O. Heinz
Department of Physics & Chemistry
Naval Postgraduate School
Monterey, California 93940

1

Dr. A. L. Slafkosky
Scientific Advisor
Commandant of the Marine Corps (Code RD-1)
Washington, D.C. 20380

1

Office of Naval Research
Arlington, Virginia 22217
Attn: Dr. Richard S. Miller

1

TECHNICAL REPORT DISTRIBUTION LIST

No. Copies

No. Copies

Dr. Paul Delahay
New York University
Department of Chemistry
New York, New York 10003

1

Library
P. R. Mallory and Company, Inc.
P.O. Box 706
Indianapolis, Indiana 46206

1

Dr. R. A. Osteryoung
Colorado State University
Department of Chemistry
Fort Collins, Colorado 80521

1

Dr. P. J. Handra
University of Southampton
Department of Chemistry
Southampton SO9 5NH
United Kingdom

1

Dr. E. Yeager
Case Western Reserve University
Department of Chemistry
Cleveland, Ohio 44106

~~Dr. Sam Perone~~
~~Purdue University~~
~~Department of Chemistry~~
~~West Lafayette, Indiana 47907~~

1

Dr. D. N. Bennion
University of California
Energy Kinetics Department
Los Angeles, California 90024

1

Dr. Royce M. Murray
University of North Carolina
Department of Chemistry
Chapel Hill, North Carolina 27514

1

Dr. R. A. Marcus
University of Illinois
Department of Chemistry
Urbana, Illinois 61801

1

Naval Ocean Systems Center
San Diego, California 92152
Attn: Technical Library

1

Dr. J. J. Auborn
Bell Laboratories
Murray Hill, New Jersey 07974

1

Dr. J. H. Ambrus
The Electrochemistry Branch
Materials Division, Research & Tech. Dept
Naval Surface Weapons Center
White Oak Laboratory
Silver Spring, Maryland 20910

1

Dr. Adam Heller
Bell Telephone Laboratories
Murray Hill, New Jersey 07974

1

Dr. G. Goodman
Glenn-Union Inc.
5757 North Green Bay Avenue
Milwaukee, Wisconsin 53201

1

Dr. T. Katan
Lockheed Missiles & Space Co., Inc.
P.O. Box 804
Sunnyvale, California 94088

1

Dr. Joseph Singer, Code 302-1
NASA-Lewis
21000 Brookpark Road
Cleveland, Ohio 44135

1

Dr. J. Boechler
Electrochimica Corporation
Attention: Technical Library
2485 Charleston Road
Mountain View, California 94040

1

Dr. S. B. Brummer
IC Corporation
15 Chapel Street
Newton, Massachusetts 02158

1

Dr. P. P. Schmidt
Oakland University
Department of Chemistry
Rochester, Michigan 48063

1

Dr. Frank Murphy
ITE Laboratories
10 Sylvan Road
Falmouth, Massachusetts 02154

1

END

FILMED

11-85

DTIC